Int J Thermophys (2007) 28:1882–1892
DOI 10.1007/s10765-007-0248-1

The Dutch National Realization of the ITS-90 over the Range 13.8033 K–273.16 K

A. Peruzzi · R. Bosma · J. van den Hark

Published online: 21 August 2007

Abstract The facility constructed at NMi VSL to realize the ITS-90 in the capsule standard platinum resistance thermometer range (CSPRT, 13.8033–273.16 K) is presented. To demonstrate the performance of our facility, the results of a recent measurement campaign are reported, in which 3 NMi VSL CSPRTs were calibrated in the range 13.8–273.16 K at all of the fixed points required by the ITS-90. The uncertainty of the calibration of the CSPRTs at each of the fixed points is evaluated in accordance with the most recent recommendations of the Consultative Committee for Thermometry and its Working Groups 1 and 3.

Keywords ITS-90 · Sealed triple-point cells · Temperature fixed points

1 Introduction

Within the framework of an EU project (MULTICELLS [1–3] from 2000 to 2003), the NMi VSL developed the capability to realize the ITS-90 in the range 13.8033–273.16 K. A bilateral key comparison between NRC and NMi VSL was recently carried out in the same temperature range (CCT-K2.3, September 2005 to April 2006, to be published) to establish the degree of equivalence between NMi VSL and the other national metrology institutes that participated in CCT-K2 (1997–1999, [4]).

In this article, we describe the facility constructed at NMi VSL to realize the ITS-90 in the CSPRT range. For the subrange from 13.8 to 273.16 K, the ITS-90 requires that the resistance of the capsule thermometer be measured at the defining fixed points of equilibrium hydrogen (13.8033 K), neon (24.5561 K), oxygen (54.3584 K),

A. Peruzzi (✉) · R. Bosma · J. van den Hark
Nederlands Meetinstituut van Swinden Laboratorium, P.O. Box 654, 2600 AR, Delft, The Netherlands
e-mail: aperuzzi@nmi.nl

argon (83.8058 K), mercury (234.3156 K), and water (273.16 K) and at two additional temperatures close to 17.0 and 20.3 K.

The cryogenic fixed points (hydrogen, neon, oxygen, and argon) are realized at NMi VSL by using state-of-the-art sealed triple-point cells (STPCs) of the corresponding high-purity gases (99.999–99.9995%) in combination with an adiabatic calorimeter. The measurements at 17.0 and 20.3 K are performed by using the same calorimeter environment (with a minor reversible modification allowed by its flexible design) and a reference temperature provided by previously calibrated rhodium-iron resistance thermometers (RIRTs). The resistance of the SPRTs at the mercury and water fixed points is measured by adapting the fixed points used to calibrate long-stem standard platinum resistance thermometers, LSPRTs (sealed mercury and water triple-point cells with corresponding maintenance baths) to the physical requirements of the CSPRTs.

To demonstrate the performance of our facility, we report the results of a recent measurement campaign in which 3 CSPRTs were calibrated in the range 13.8–273.16 K. The uncertainty budget for each of the defining fixed points is evaluated in accordance with the most recent recommendations of the Consultative Committee for Thermometry and its Working Groups 1 and 3.

2 Experimental

2.1 Cryogenic Fixed Points

2.1.1 Experimental Setup

The ITS-90 cryogenic fixed points (e-H_2, Ne, O_2, and Ar) are realized in sealed triple-point cells (STPCs) by adiabatic calorimetry [5,6]. Four STPCs (each one containing a different gas and, thus, realizing a different fixed point) and the CSPRTs to be calibrated (up to 5) are mounted in a copper block (see Fig. 1). The copper block is suspended from the copper flange of the calorimeter by a Teflon frame and enclosed within a temperature-controlled copper shield and the stainless steel vacuum chamber of the calorimeter. The calorimeter is inserted in a cryostat filled with the appropriate cryogenic liquid necessary to solidify the gas in the STPC: liquid helium when realizing the H_2 and Ne triple points, and liquid nitrogen when realizing the O_2 and Ar triple points. Liquid nitrogen is pumped down to 48 K when realizing the O_2 triple point.

A schematic view of the experimental setup is shown in Fig. 2. After solidifying the gas in the STPC selected for the measurement, the copper block is thermally isolated by removing the exchange gas from the vacuum chamber and the temperature of the copper shield is controlled at a few millikelvin above the corresponding triple-point temperature. Control of the copper shield temperature is realized by using a Lakeshore 340 temperature controller, a manganin heater wound and glued around the external lateral surface of the shield, and two thermometers (one Pt100 and one germanium) attached to the shield.

Measured current pulses are then applied to the manganin heater on the copper block, alternating with recovery periods, which first drive the sample into the

Fig. 1 The four stainless-steel sealed triple-point cells (H_2, Ne, O_2, and Ar, of which only two are visible) and five capsule standard platinum resistance thermometers mounted in the copper block. The manganin heater wound around the lateral surface of the copper block is also visible. The copper block is shown attached to the cryostat, prior to mounting the copper shield and the stainless steel vacuum chamber

solid–liquid transition and then progressively melt the substance. The copper block heater is powered by a Keithley 224 current source. A HP3458A multimeter and a HP34420A nanovoltmeter are used to measure, respectively, the current and the voltage across the heater.

The CSPRT resistance is measured by using an ASL F-18 resistance bridge in combination with a standard resistor (Tinsley, Type 5685A) selected from a set of four (1, 10, 25, and 100 Ω nominal values) immersed in a temperature-controlled oil bath (stability 1 mK).

2.1.2 Ancillary Calculations and Measurements

Based on knowledge of the amount of gas in each cell (provided by the manufacturer, INRIM, formerly IMGC, Torino, Italy) and the latent heat of fusion of each gas (from the literature), the enthalpy of fusion is calculated for each cell (see Table 1).

A protocol [7] is followed in performing the measurements which requires the preliminary investigation of the thermal behavior of the STPC by evaluating the following quantities:

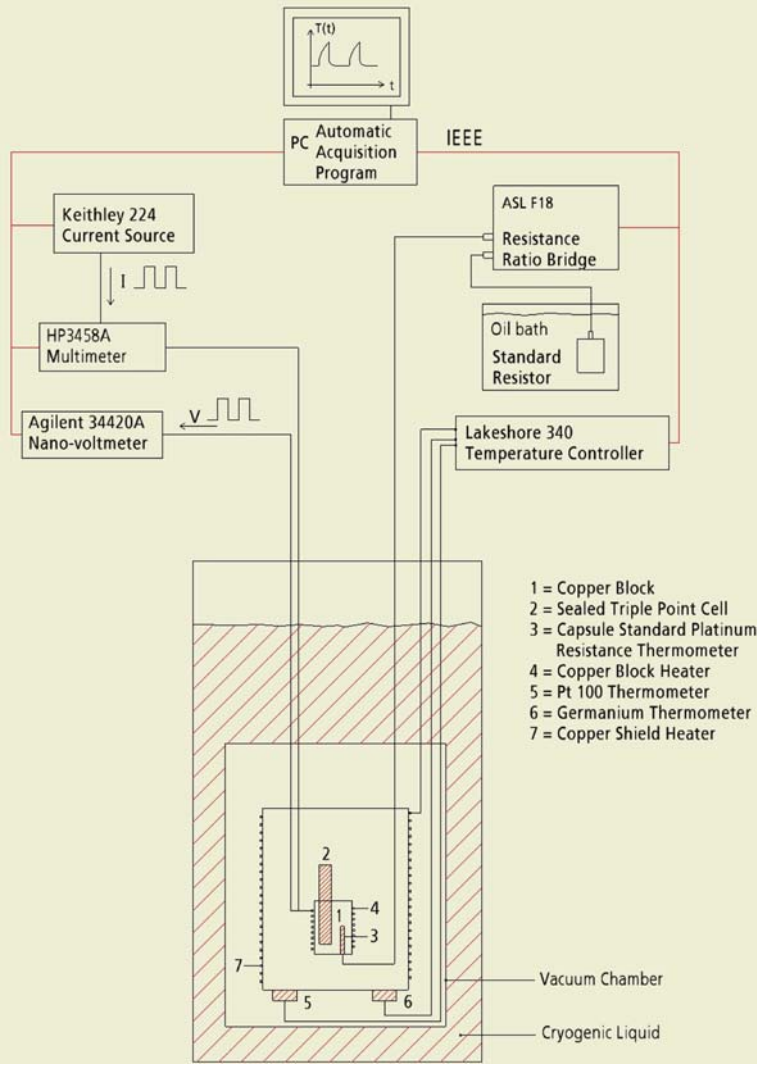

Fig. 2 Schematic view of the experimental setup for the realization of the cryogenic fixed points

- Thermal resistance $R_{CS}(F)$ between the solid–liquid interface and the CSPRT as a function of the melted fraction F.
- Heat capacity C of the calorimeter (copper block + STPCs + CSPRTs) outside (but very close to) the melting plateau.
- Initial temperature overheating ΔT_{CS} after a pulse.

These quantities are then used to estimate the maximum allowed heat leak $P_{\text{leak}}^{\text{Max}}$, the maximum allowed temperature drift $(\mathrm{d}T/\mathrm{d}t)^{\text{Max}}$ close to the melting plateau, and the minimum recovery time $\tau_{\text{recovery}}^{\text{Min}}$ after a pulse, to ensure that the maximum static and dynamic temperature measurement errors do not exceed the specified values of

Table 1 Summary of the information available for each STPC before starting the measurements

Fixed Point	Identification number	Date of production	Amount of substance (mol)	Latent heat of fusion ($J \cdot mol^{-1}$)	Total enthalpy (J)
Ar (83.8058 K)	E2Ar	2000/09/08	0.1022	1189	121.5
O_2 (54.3584 K)	Eb2/O2	2001/06/08	0.0875	444	38.9
Ne (24.5561 K	E3Ne	2000/09/29	0.0845	335	28.3
H_2 (13.8033 K)	Eb1H2	2001/03/12	0.0655	117	7.7

Table 2 Typical numerical values of the cell parameters (columns 2, 3, and 4), the calorimeter environmental conditions (columns 5, 6, and 7), and the corresponding observed experimental conditions (columns 8, 9, and 10)

STPC	R_{CS}^{Max} ($K \cdot W^{-1}$)	C ($J \cdot K^{-1}$)	ΔT_{CS} (mK)	P_{leak}^{Max} (μW)	$(dT/dt)^{Max}$ ($mK \cdot h^{-1}$)	$\tau_{recovery}^{Min}$ (s)	P_{leak} (μW)	(dT/dt) ($mK \cdot h^{-1}$)	$\tau_{recovery}$ (s)
Ar	2.2	115	49	9	0.3	1, 974	2.2	0.07	3,600
O_2	1.5	65	19	13	0.7	669	0.9	0.05	3,600
Ne	2	12	61	10	3	179	2.5	0.7	7,000
H_2	20	5	76	1	0.7	824	0.4	0.3	7,000

ΔT_{Static}^{Max} and $\Delta T_{Dynamic}^{Max}$, respectively:

$$P_{leak}^{Max} = \left(\Delta T_{Static}^{Max} / R_{CS}^{Max}\right)$$
$$P_{leak}^{Max} = C\,(dT/dt)^{Max}$$
$$\tau_{recovery}^{Min} = R_{CS} C \ln\left(\Delta T_{CS} / \Delta T_{Dynamic}^{Max}\right)$$

where R_{CS}^{Max} is the maximum value of $R_{CS}(F)$ over the range $0 < F < 1$.

Table 2 summarizes the measured values of the cell parameters (columns 2, 3, and 4), the requirements imposed on the calorimeter environment in order to maintain both the static and dynamic temperature measurement errors less than 20 μK (columns 5, 6, and 7), and the corresponding experimental conditions (columns 8, 9, and 10).

The actual recovery time $\tau_{recovery}$ was prudentially selected much larger than the minimum required $\tau_{recovery}^{Min}$ (compare column 7 with column 10 of Table 2) because the thermal model adopted is usually less than satisfactory.

2.1.3 Automatic Measurement Acquisition Program

An automatic acquisition program was implemented in Borland Delphi 5[1] to perform the resistance measurements of the CSPRTs along the melting plateau. By inserting a number of input parameters, the desired measurement pattern can be selected. A

[1] Inprise Corporation, 100 Enterprise Way, Scotts Valley, CA 95066–3249, USA.

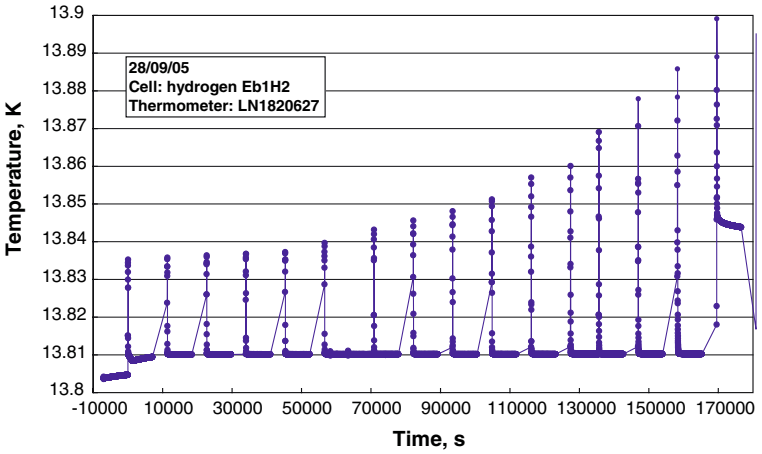

Fig. 3 A two-day long hydrogen measurement. During the heat pulse and recovery periods, the temperature is monitored with one of the CSPRTs to be calibrated. Notice the jump of about one hour at the end of each recovery period, during which all CSPRT resistances are automatically measured and stored in the database

measurement pattern (see Fig. 3) is a sequence of N (with typically $N = 10$ or 20) repeated identical cycles, each cycle being composed of three subsequent parts;

1. Heat pulse, in which a current i_{pulse} is applied to the heater of the copper block for a period τ_{pulse}, and a relevant fraction of the solid is melted (typically 10 or 5%).
2. Recovery period τ_{recovery}, in which thermal equilibrium is recovered between the STPCs, the CSPRTs, and the copper block (more exactly, a stationary condition is reached in which temperature gradients between different parts of the system become negligible).
3. Measurement, in which the resistances R_k of the CSPRTs are measured using the resistance bridge and the standard resistor R_k^{S}. For each CSPRT, the bridge parameters (the measuring current i_k, the measuring frequency f_k, the bandwidth BW_k, the gain G_k, and the quadrature gain Q_k) can be selected independently. The zero-current resistance R_k of each CSPRT is obtained from a cycle of 90 real measurements: 30 measurements at a current i_k, 30 measurements at a current $i_k\sqrt{2}$, and again 30 measurements at a current i_k.

2.1.4 Data Analysis

For each cryogenic fixed point, at least three plateaux are measured. For each plateau at a given fixed point, the resistance $R_k(F)$ of each CSPRT is plotted as a function of the melted fraction F (see Fig. 4). The graphical representation allows the resistance value of the CSPRT corresponding to the liquidus point, $R_k(F = 1)$, to be identified by extrapolation, within a statistical uncertainty of a few tenths of microkelvin.

The resistance value of a CSPRT at a given fixed point is then assumed to be the average of the $R_k(F = 1)$ obtained for all the plateaux realized under the required

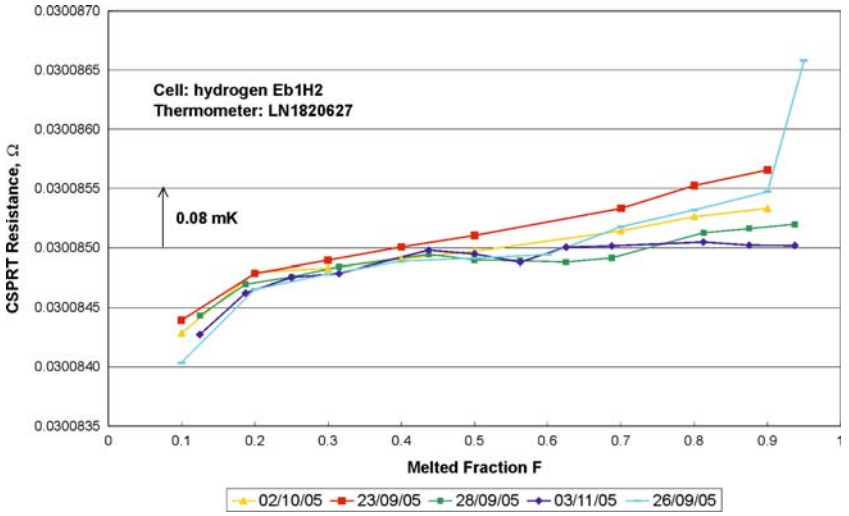

Fig. 4 Hydrogen plateaux measured with thermometer Leeds and Northrup 1820627. Note that the resistance value at the liquidus point is different from the one reported in Table 3 because it has not been corrected for the isotopic composition

conditions. For the case of the hydrogen fixed-point cell, the average value is then corrected for the isotopic composition of the sample.

2.2 Additional Temperatures Close to 17.0 and 20.3 K

For the two additional temperatures close to 17.0 and 20.3 K, the CSPRTs were calibrated by comparison with two 100 Ω rhodium-iron thermometers (identification numbers 226246 and 229080), mounted on the same copper block as the CSPRTs. Thermometer 226246, the same used in CCT-K1 [8], carries the NMi VSL gas thermometer scale [9]. Thermometer 229080 carries the NPL-75 gas thermometer scale. More details about the history of these two thermometers can be found in [10].

The reference temperature was defined as the average of the temperatures given by the NPL-75 and NMi VSL gas thermometer scales. The difference between the two scales was 0.18 mK at both 17.0 and 20.3 K (with NPL-75 "hotter" than the NMi VSL scale).

Note that, in this case, the copper shield and the copper block played different roles with respect to their roles in the cryogenic fixed-point measurements:

- In the fixed-point measurements, the thermal 'source' with which the copper block (and the thermometers attached to it) is brought into equilibrium is the phase transition itself (the solid–liquid interface).
- In the 17.0 and 20.3 K measurements, the thermal 'source' is the copper shield, whose temperature is controlled close to the required nominal values of 17.0 and 20.3 K. The copper block holding the thermometers will try to follow the copper shield temperature.

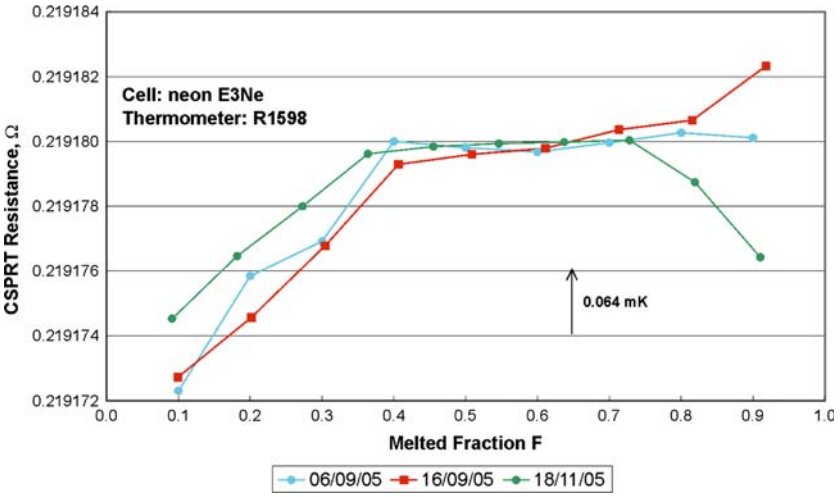

Fig. 5 Neon plateaux measured with thermometer Rosemount 1598

2.3 Mercury and Water Fixed Points

The measurements of the CSPRTs' resistances at the mercury and water triple points were performed using the same instrumentation (cells and maintenance baths) used to calibrate long-stem standard platinum resistance thermometers (LSPRTs). To establish good thermal contact between the CSPRT and the fixed-point cell, the thermometer well of the fixed-point cell was filled with a very-low viscosity silicone oil intended for low-temperature applications (Kryo 85).

3 Measurement Results

The melting plateaux of selected CSPRTs, in the form of their resistance $R_k(F)$ as a function of the melted fraction F, are reported in Figs. 4–7. The spread between the melting curves increases substantially at low and high F values because, for $F < 0.2$ and $F > 0.8$, the system is highly sensitive to the thermal environment.

Before performing the measurements at 17 and 20.3 K, the thermal contact between the copper block and the copper shield was improved by replacing the manganin leads with Cu leads. To investigate how the thermal environment affects the melting curves, the measurements at the four cryogenic fixed points were repeated with the modified thermal contact. The results obtained with the modified thermal contact were families of melting plateaux slightly shifted down with respect to the previous measurements. This can be clearly seen in Figs. 6 and 7.

The total electrical energy supplied to the sample during melting agrees with the expected enthalpy given in Table 1 within a few percent (3–5%), the difference being due to the thermal leak of the calorimeter.

The resistance values of three CSPRTs at all of the fixed points, corrected for self heat, hydrostatic head, and isotopic effects, are reported in Table 3.

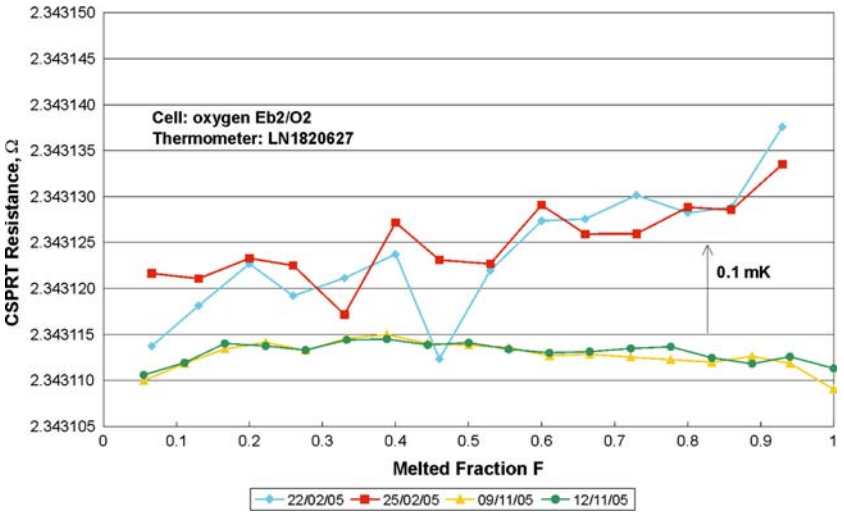

Fig. 6 Oxygen plateaux measured with thermometer Leeds and Northrup 1820627. Two additional measured plateaux are not plotted in the figure, but the corresponding extrapolated liquidus points were used to calculate the average liquidus point reported in Table 4

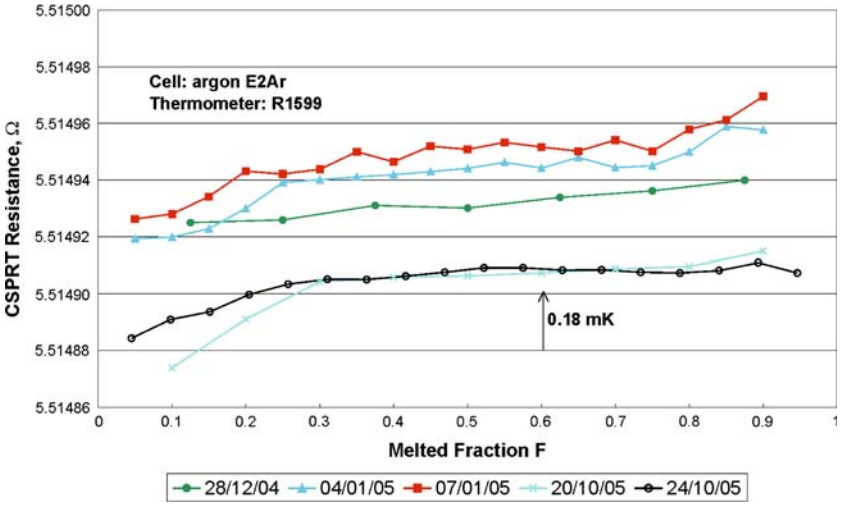

Fig. 7 Argon plateaux measured with thermometer Rosemount 1599

4 Isotopic and Impurity Effects on the Realized Triple-Point Temperatures

The values of the CSPRT resistances measured for e-H_2 and H_2O were corrected for the respective isotopic compositions.

The deuterium concentration in the hydrogen cell (Eb1H2) is (45.8 ± 0.3) µmolD/molH. Using the depression constant $k_D = (5.42 \pm 0.31)$µK/(µmolD/molH) suggested by Fellmuth [11], a correction of +234 µK was applied for hydrogen.

Table 3 Resistance values of three CSPRTs measured at the fixed points, corrected for self heating, hydrostatic head, and isotopic effects

Fixed-Point Temperature (K)	Rosemount 1598 (Ω)	Rosemount 1599 (Ω)	Leeds and Northrup 1820627 (Ω)
273.16	25.53776478	25.53351270	25.54376539
234.3156	21.55802546	21.55453009	21.56262025
83.8058	5.51541712	5.51492969	5.51424036
54.3584	2.34560361	2.34574254	2.34313810
24.5561	0.219180058	0.219785866	0.215722908
20.28222	0.11167384	0.11229786	0.10822084
16.98826	0.06123677	0.06185661	0.057849941
13.8033	0.033332343	0.033927902	0.030086886

The isotopic analysis of the water contained in the water cell (VSL03T026) gave:
$\delta^2\mathrm{H} = (-51.1 \pm 0.8)‰$ (coverage factor $k = 1$)
$\delta^{18}\mathrm{O} = (-6.93 \pm 0.08)‰$ (coverage factor $k = 1$)
with $\delta^2\mathrm{H}$ and $\delta^{18}\mathrm{O}$ the deviations of $^2\mathrm{H}$ and $^{18}\mathrm{O}$ content with respect to VSMOW (Vienna Standard Mean Ocean Water) as defined in [12]. Using the depression constants recommended in [12], a correction of +37 μK was applied. The temperature corrections were transformed into resistance corrections using the known sensitivity of each CSPRT.

The impurity content was insufficiently known to apply corrections. The total impurity concentration was used with the first cryoscopic constant to estimate the uncertainty due to the presence of impurities (overall maximum estimate, see [13]).

5 Uncertainties

The uncertainty budget for the calibration of CSPRTs at fixed points in the range 13.8–273.16 K is reported in Table 4. The origin of each uncertainty component is identified in the table itself. Most of the uncertainty sources are self-explanatory and do not require further discussion.

The uncertainty of the reference scale at 17.0 and 20.3 K was assumed to be the average of the uncertainties of the NPL-75 and NMi VSL gas thermometer scales.

The uncertainty arising from the hydrostatic head effect is evaluated for the cryogenic fixed points by assuming an uncertainty of 2 cm for e-H_2 and 1 cm for Ne, O_2, and Ar in the location of the solid–liquid interface within the sealed cell.

The reproducibility is calculated as the standard deviation of the mean of the resistance values obtained for all the measured plateaux, averaged over all measured thermometers.

The standard combined uncertainty at the fixed points ranges from about 70 μK at the hydrogen fixed point to 200 μK at the 17 and 20.3 K points.

6 Conclusions

We described the realization of the ITS-90 in the capsule-type SPRT range (13.8033–273.16 K) at NMi VSL. The same facility is used to disseminate the scale by calibrating

Table 4 Uncertainty budget for the calibration of CSPRTs at fixed points in the range 13.8–273.16 K. All uncertainties are expressed in μK with a coverage factor $k = 1$

Uncertainty component ($k = 1$)	e-H_2	17 K	20 K	Ne	O_2	Ar	Hg	H_2O
Isotopic composition	14	–	–	157	0	0	0	1
Chemical impurities	20	–	–	30	50	10	12	69
Liquidus point identification	30	–	–	50	40	50	58	10
Reference scale (ICVGT)	–	200	200	–	–	–	–	–
Hydrostatic head correction	5	–	–	19	15	33	74	8
Self-heat correction	23	30	30	30	34	20	30	23
Residual gas pressure	0	–	–	0	0	0	0	3
Static temperature measurement error	20	–	–	20	20	20	–	–
Dynamic temperature measurement error	20	–	–	20	20	20	–	–
Temperature drift correction	–	53	25	–	–	–	–	–
Standard resistor	1	1	1	1	4	7	35	41
Resistance ratio bridge	80	80	80	80	4	4	14	15
WTP propagation	2	2	2	2	8	17	73	–
Reproducibility	46	–	–	46	139	52	50	26
Standard combined ($k = 1$) uncertainty	107	224	219	196	160	87	138	90

customer thermometers, either directly against the fixed-point cells or against CSPRTs previously calibrated at the fixed points. This dissemination scheme, together with the publication of the results of the CCT-K2.3 comparison, will support improved CMC entries for NMi VSL.

Acknowledgments This work was supported in part by the European Commission under Contract No. G6RD-CT-1999-00114. The authors would like to thank Maurice Heemskerk for the drawing of Fig. 2.

References

1. F. Pavese, B. Fellmuth, D. Head, Y. Hermier, A. Peruzzi, A. Szmyrka Grzebyk, L. Zanin, in *Temperature: Its Measurement and Control in Science and Industry*, vol. 7, Part 1, ed. by D.C. Ripple (AIP, New York, 2003), pp. 161–166
2. F. Pavese, D. Ferri, I. Peroni, A. Pugliese, P.P.M. Steur, B. Fellmuth, D. Head, L. Lipinski, A. Peruzzi, A. Szmyrka Grzebyk, L. Wolber, in *Temperature: Its Measurement and Control in Science and Industry*, vol. 7, Part 1, ed. by D.C. Ripple (AIP, New York, 2003), pp. 173–178
3. Y. Hermier, L. Pitre, C. Geneville, A. Verge, G. Bonnier, D.I. Head, B. Fellmuth, L. Wolber, A. Szmyrka-Grzebyk, L. Lipinski, M.J. de Groot, A. Peruzzi, in *Temperature: Its Measurement and Control in Science and Industry*, vol. 7, Part 1, ed. by D.C. Ripple (AIP, New York, 2003), pp. 179–184
4. A.G. Steele, B. Fellmuth, D.I. Head, Y. Hermier, K.H. Kang, P.P.M. Steur, W.L. Tew, Metrologia **39**, 551 (2002)
5. J. Ancsin, Metrologia **9**, 147 (1973)
6. F. Pavese, Metrologia **14**, 93 (1978)
7. B. Fellmuth, L. Wolber, Protocol for the investigation of the thermal properties of multicells, *Report EU project MULTICELLS* (Contract No. GRD1-1999-10423), Physicalisch-Technische Bundesanstalt (PTB), Berlin, Germany
8. R. Rusby, D. Head, C. Meyer, W. Tew, O. Tamura, K. Hill, M.J. de Groot, A. Storm, A. Peruzzi, B. Fellmuth, J. Engert, D. Astrov, Y. Dedikov, G. Kytin, Metrologia **43**, Tech. Suppl. 03002 (2006)
9. P.P.M. Steur, M. Durieux, Metrologia **23**, 18 (1986)
10. M.J. de Groot, J. Mooibroek, P. Bloembergen, M. Durieux, A. Reesink, M. Yuzhu, *Proc. TEMPMEKO '93, 5th Int Symp. on Temperature and Measurement in Industry and Science* (1993), pp. 90–95
11. B. Fellmuth, L. Wolber, F. Pavese, P.P.M. Steur, I. Peroni, A. Szmyrka-Grzebyk, L. Lipinski, W.L. Tew, T. Nakano, H. Sakurai, O. Tamura, D. Head, K.D. Hill, A.G. Steele, Metrologia **42**, 171 (2005)
12. *CCT document CCT/05–07*, BIPM, Paris (2005)
13. *CCT document CCT/05–08*, BIPM, Paris (2005)